Stimulated-photon-echo spectroscopy. I. Spectral diffusion in Eu^{3+}:$YAlO_3$

Ryuzi Yano, Masaharu Mitsunaga, and Naoshi Uesugi
NTT Basic Research Laboratories, Musashino-shi, Tokyo 180, Japan
(Received 8 April 1991; revised manuscript received 26 August 1991)

Systematic measurements of stimulated-photon-echo intensities as a function of the first-to-second (τ) and second-to-third (T) pulse separations allow the investigation of the dynamical properties of the spectral diffusion for the $^7F_0$-$^5D_0$ transition of a cryogenic Eu^{3+}:$YAlO_3$ sample. The existence of spectral diffusion was verified by the significant broadening (from 1.2 to 7.2 kHz) of the homogeneous linewidth (Γ) as T increases from microseconds to milliseconds, the effect being attributed to the flip flop of nearby aluminum nuclear spins surrounding the Eu^{3+} ion. A similar broadening effect (from 0.61 kHz, to a few kHz) was also observed in the presence of a static magnetic field $H_0=137$ G, but with a much slower diffusion rate. To explain these observations, we use three theoretical models: the Bai-Fayer model, the diffusion-equation model, and the Monte Carlo model. Each agrees reasonably well with the experimental data and indicates the flip rates of sub-kHz order at $H_0=0$ and an order of magnitude lower at 137 G.

I. INTRODUCTION

In studying the excited-state dynamics of rare-earth ions doped in crystals, photon-echo spectroscopy[1-5] is one of the most common methods. Specifically, as shown in the following, an analysis of the stimulated photon echo (SPE) provides far more information than does the ordinary two-pulse photon echo (TPPE) technique. In a typical SPE experiment as illustrated in Fig. 1(a), one applies three successive resonant optical pulses to a sample and observes the SPE as a coherent response signal. Unlike TPPE, the SPE measurement involves two parameters that can be independently varied: the first-to-second pulse separation τ, and the second-to-third pulse separation T. A systematic SPE experiment with various τ and T therefore enables us to obtain a three-dimensional plot of SPE intensity vs τ and T, as exemplified in Fig. 1(b).

A number of important physical mechanisms can be extracted from this plot: (1) The (intrinsic) dephasing time T_2 is determined from the SPE decay time along the τ axis at $T=0$. This automatically yields the (intrinsic) homogeneous linewidth Γ in the limit of no spectral diffusion by the relation $\Gamma=1/\pi T_2$. (2) The leading part of the SPE decay along the T axis at $\tau=0$ represents the excited-state lifetime T_1, since no grating is formed in the absorption spectrum. (3) In general, the SPE signal does not disappear even when $T\gg T_1$ because the recovery of the ground-state population to the original thermal equilibrium takes a much longer time, given by the ground-state sublevel (e.g., hyperfine level) lifetime T_{sub}. Hence, the SPE decay along the T axis in a long-time range gives T_{sub}. (4) The effect of spectral diffusion can be studied by the shortening of the dephasing time T_2 (SPE decay time along the axis τ) or, equivalently, the broadening of the homogeneous linewidth Γ as T increases. (5) If the system has a sublevel structure in the ground state and/or the excited state, the SPE intensity will be modulated along both τ and T as shown in Fig. 1(b). This modulation originates from the interference effect among dipole moments connecting different sublevels, and will be discussed in detail in the following paper.[6] In this case, the ground-state and/or excited-state sublevel splitting frequencies will be the SPE modulation frequencies. (6) Similarly, the inhomogeneous widths of these sublevel transition frequencies are measured from the decays of the corresponding oscillatory components along τ or T.

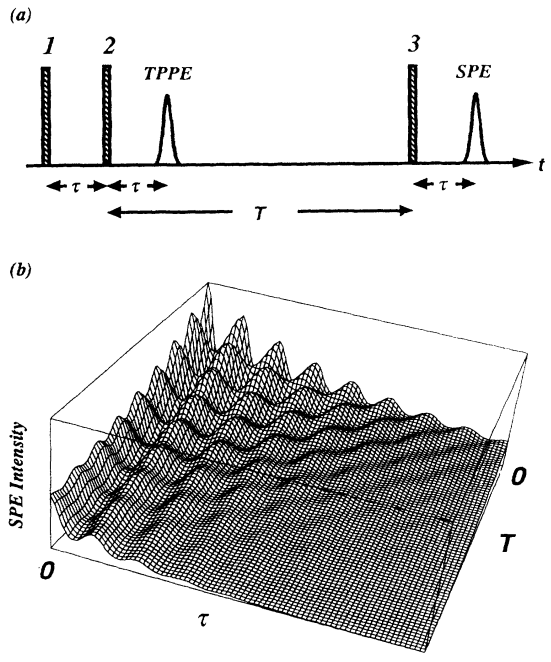

FIG. 1. (a) Excitation and response in stimulated-photon-echo experiments. τ, first-to-second pulse separation; T, second-to-third pulse separation. The echo signal is formed at time τ after the third pulse. (b) Example of three-dimensional plot of stimulated-photon-echo intensity as a function of τ and T.

Aside from these items, the coherent dynamical property of the material will be visualized and directly understood from a three-dimensional plot like Fig. 1(b). This SPE spectroscopy is especially powerful for studying spectral diffusion and photon-echo modulation since these two cases require measurement of the SPE intensity dependences on both τ and T.

Here and in the following paper[6] we present two typical applications of this technique. In this paper we introduce the experimental apparatus for SPE spectroscopy and study the effect of spectral diffusion in Eu^{3+}:$YAlO_3$. The shortening of the dephasing time with increasing T is indeed pronounced, which helps to study the microscopic diffusion dynamics of this sample. To interpret these experimental results, three theoretical approaches are presented and each approach is compared with the observations. The following paper treats the problem of the photon-echo modulation in Pr^{3+}:$YAlO_3$. Since echo-modulation periods are much longer in Pr^{3+}:$YAlO_3$ than in Eu^{3+}:$YAlO_3$, a Pr sample gives the more pronounced modulation effect when the experimental time resolution (pulsewidths) is very poor. There the echo-modulation theory in the presence of sublevels is developed and is compared three-dimensionally with the experimental results.

In closing the introduction section, it should be emphasized that this study is also important from the viewpoint of time-domain optical memory[7-11] because each SPE decay curve with a fixed T (readout time, in terms of optical memory) corresponds to the envelope of the readout data. It is desirable that the envelope should not have any modulation or shortening of the decay time, since the output data should not depend on the readout time T. This SPE spectroscopy visually gives the correct information of the output data wave form for a given T value.

II. APPARATUS

Figure 2 shows a schematic diagram of the apparatus for SPE spectroscopy. A linearly polarized cw ring dye laser (Coherent: CR-699-21) oscillating in the locked mode (~5 MHz linewidth) is used for the excitation source of the sample. The output of the dye laser is divided by a beam splitter and its wavelength and frequency spectrum are monitored by a wavemeter (Advantest: TQ8325) and a spectrum analyzer (Newport: SR-130).

Three excitation pulses for the SPE experiment are generated by gating the cw beam with two acousto-optic modulators (AOM's) (Matsushita: EFL-M200) placed in tandem. We first tried to observe photon echoes by using only one AOM, but could not. There was a constant leak, about $\frac{1}{1000}$ of the excitation beam intensity, in the direction of the excitation beam. This leaked beam, we believe, degraded the coherence of the macroscopic dipole moment of the sample and diminished the echo signal. And, what was worse, the echo signal was homodyne detected by the leaked beam. Since the relative phase between the echo signal and the leaked beam was not fixed, the echo signal randomly shifted between positive and negative. These problems were overcome by using two AOM's.

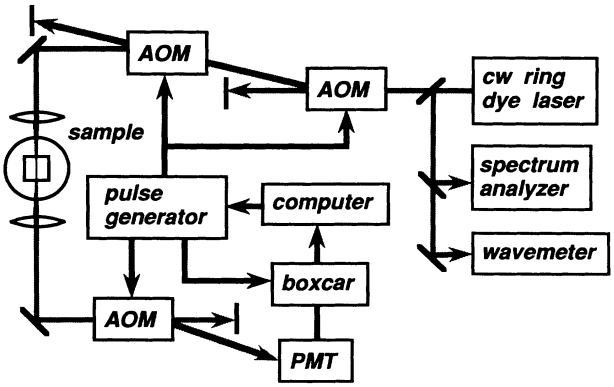

FIG. 2. Schematic diagram of apparatus for stimulated-photon-echo spectroscopy. AOM, acousto-optic modulator; PMT, photomultiplier tube.

There are several advantages of employing gated-cw pulses instead of low-repetition-rate pulsed lasers in SPE spectroscopy. Owing to the long-time high-intensity stability of the cw ring dye laser, the signal-to-noise (S/N) ratio of the echo signal is highly improved. Arbitrary pulse separations, τ and T, are easily made by the use of the AOM's. These two factors altogether enable SPE spectroscopy with systematic variation of τ and T. If pulsed dye lasers were used as excitation light source for rare-earth ions in crystals, three independently triggered pulsed lasers or two impractically long optical delay lines would be needed. Furthermore the S/N ratio of the echo signals would be low due to the large intensity fluctuation of the pulsed lasers.

The excitation beams are focused by a lens on the sample in a gas-flow-type cryostat (Oxford: CF1204). In this configuration, both the echo signal and the excitation beams propagate in the same direction. The AOM in front of the photomultiplier tube (PMT) (Hamamatsu Photonics: R3824) works as an optical shutter, opening only when the echo signal enters the AOM. The echo signal is diffracted by the AOM and detected by the PMT. The detected signal is averaged by a boxcar integrator (Stanford Research Systems: SR250) and is stored in a personal computer. The timing of the excitation pulses, the optical shutter, and the trigger pulse for the boxcar integrator is controlled by the personal computer through the pulse generator (Stanford Research Systems: DG535). This fully computerized SPE measurement takes about 30 min in a typical run to obtain a three-dimensional plot (100×100 data points) such as that shown in Fig. 1(b).

III. EXPERIMENT

A. Motivation

There are many different techniques for measuring dephasing times: optical hole burning,[12] holographic hole burning,[13,14] fluorescence line narrowing,[15] delayed free

induction decay (FID),[16,17] photon echo,[1-5] accumulated photon echo,[18] incoherent light photon echo,[19-23] and so on. Recent studies have shown that these techniques do not necessarily give the same dephasing time due to the different time scales of their measurements,[24-28] which leads to intrinsic dephasing and spectral diffusion. Here the term intrinsic dephasing refers to the dephasing caused by only $\sim 1/T_2(T\rightarrow 0)$ rate fluctuations, where $T_2(T\rightarrow 0)$ is the dephasing time measured by TPPE, and not to those caused by slow rate fluctuations such as spectral diffusion. To avoid confusion, the term (optical) dephasing will be applied to the dephasing that is measured by SPE and that is caused by both $\sim 1/T_2(T\rightarrow 0)$ rate fluctuations and slow rate fluctuations.

There are many studies of intrinsic dephasing and spectral diffusion for chromophores in glasses at low temperatures.[24-31] Both of these phenomena in glasses are considered to be caused by the local configurational changes of the materials.[32] These configurational changes are often modeled by the two-level systems (TLS's) proposed by Anderson, Halperin, and Varma[33] and Philips[34] to explain the anomalous specific-heat capacities of glasses at low temperatures.

There are a few studies, however, of these phenomena at low temperatures for rare-earth ions or transition-metal ions in crystals.[17,27,35,36] The intrinsic dephasing and spectral diffusion in rare-earth ions or transition-metal ions in crystals at low temperatures are usually considered in the following.[37-40] The local-field fluctuation due to mutual flips of the nuclear spins of the bulk causes intrinsic dephasing. On the other hand, the nearby nuclear spins surrounding the optical center are detuned from the bulk nuclear spins by the strong local magnetic field created by the optical center. Thus their flip rates are slowed down and they form a frozen core. These nearby nuclear spins cause spectral diffusion. In the case of Eu^{3+}:$YAlO_3$, it is probable that the nearby Al spins which surround a Eu ion form a frozen core by the perturbed electric field gradient at the Al site because of the ionic radii mismatch between Eu and Y.[41,42]

In the recent study of accumulated photon echoes, we obtained an evidence which suggests the existence of spectral diffusion for the $^7F_0$-$^5D_0$ transition (581.6 nm) of Eu^{3+}:$YAlO_3$ at low temperatures.[10] In the present study, we performed SPE spectroscopy systematically and obtained a clear evidence of spectral diffusion in Eu^{3+}:$YAlO_3$.

Delayed FID and time-resolved hole burning can also be employed for the measurement of spectral diffusion, but SPE spectroscopy has several advantages over these methods. Both delayed FID and time-resolved hole burning require a laser beam with a spectral width much narrower than the holewidth and with an excitation intensity low enough to avoid an artificial broadening of a hole. SPE spectroscopy is, in principle, free from these limitations and the second-to-third pulse separation T can be varied in a wide range (from $T<T_2$ to $T\sim$ ms or more)—i.e., as far as the photon echo can be observed. As will be shown, a wide range of spectral diffusion phenomenon can be mapped out by using SPE spectroscopy.

B. Procedure

Since the basic procedure for measuring the SPE was already given in Sec. II, we will mention here only some experimental parameters and important points in performing SPE spectroscopy for Eu^{3+}:$YAlO_3$. The sample was 0.25 at. % Eu^{3+}:$YAlO_3$ ($5\times 5\times 10$ mm^3). The approximately 40-mW beam from the dye laser excited the $^7F_0$-$^5D_0$ transition (581.6 nm) of the sample at ~ 5.5 K. Transmission of the excitation beam was about 35% at this transition.

Recently it has been reported for rare-earth ion in crystals that the dephasing time measured by TPPE becomes shorter when the excitation intensity is increased.[43-45] This effect is attributed to the sudden change of optical transition frequency of a given Eu ion due to the sudden change of the local field when neighboring Eu ions are optically excited. This phenomenon has been also observed in our sample.[10] To eliminate this effect, we performed SPE spectroscopy at a low excitation limit, setting the width of each excitation pulse at 0.5 μs and using a soft-focusing lens to focus the beam on the sample. Considering the S/N ratio of the echo decay curves, only when the second-to-third pulse separation T was 5 ms, did we use 1-μs pulses. We also checked that the intrinsic dephasing time did not decrease if we changed all the pulse widths around 1 μs.

Eu^{3+}:$YAlO_3$ is known to have a long hole recovery time ($\sim$ hours) because of its long ground-state hyperfine level lifetime at low temperatures.[46] The frequency of the dye laser was scanned at a rate of ~ 0.15 GHz/s over a 0.3-GHz scan width, and the excitation pulse sequence was typically repeated at a rate of 80 Hz to avoid the complications due to persistent hole burning. We observed no echoes produced by previous excitation pulse sequences.

Intrinsic dephasing times of rare-earth ions or transition-metal ions in crystals measured by TPPE are well known to increase when a static magnetic field is applied to the sample.[37,48,49] A static magnetic field is also expected to affect the spectral diffusion phenomenon. We also measured systematically SPE dephasing times when a static magnetic field $H_0=137$ G was applied perpendicular to the c axis of the sample.

C. Results

Echo decay curves were well fitted by a single exponential decay at τ from 0 to ~ 100 μs. We assume in the following that echo decay curves are expressed by a single exponential decay. Figure 3 shows the three-dimensional plot of SPE spectroscopy in Eu^{3+}:$YAlO_3$ with $H_0=0$ at 5.5 K, τ varied from 4 to 100 μs and T from 2 μs to 1 ms. The main contribution of the echo intensities for $T<T_1$ is the transient population gratings of both the excited and ground states. When $T>T_1$, on the other hand, the echo signals are created mainly by the population grating of the ground-state hyperfine levels.[18,47] The echo intensities at $\tau=T=40$ and 80 μs are accidentally enhanced by the overlap of the TPPE created by the second and third pulses, and by the SPE. This three-dimensional plot

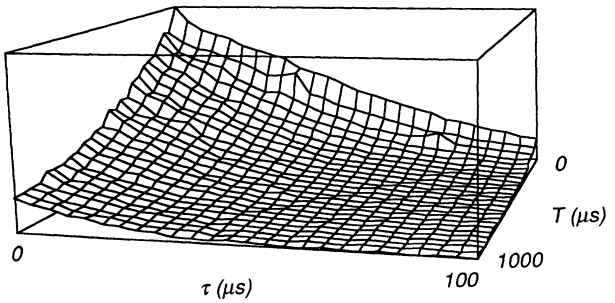

FIG. 3. Three-dimensional plot of stimulated-echo intensity (arbitrary units) vs τ and T for the $^7F_0$-$^5D_0$ transition of Eu^{3+}:$YAlO_3$ at ~5.5 K with $H_0=0$.

clearly shows that the dephasing time T_2 becomes shorter as T becomes longer.

In a separate experiment, the dephasing time T_2 dependence on T with and without a static magnetic field H_0 was measured by varying T between 2 μs and 5 ms. In our notation, homogeneous linewidth $\Gamma=1/\pi T_2$ corresponds to $\frac{1}{2}$ of the holewidth [full width at half maximum (FWHM)] measured by time-resolved hole burning[35,36] with the burn-to-probe time separation equal to T.[39] Figure 4 plots Γ vs T for $H_0=0$ and $H_0=137$ G to clarify the effect of a static magnetic field on the spectral diffusion phenomenon. Circles represent Γ with $H_0=0$, and squares represent Γ with $H_0=137$ G.

With $H_0=0$, the homogeneous linewidth Γ becomes from 1.2 to 7.2 kHz as T increases, i.e., spectral diffusion increases Γ about sixfold. Figure 4 also shows that the spectral diffusion phenomenon tends to plateau, with Γ reaching a maximum value at $T\approx 5$ ms. With a static magnetic field $H_0=137$ G applied perpendicular to the c axis of the sample, the intrinsic homogeneous linewidth $\Gamma(T\rightarrow 0)$ of 0.61 kHz was obtained, which we believe is the narrowest ever reported.

Both the intrinsic homogeneous linewidth $\Gamma(T\rightarrow 0)$ and spectral diffusion are affected by the presence of the static magnetic field. It is obvious that the rate of spectral diffusion and/or the broadening of the linewidth due to spectral diffusion decrease in the magnetic field. This means that the origin of the spectral diffusion is not Eu-Eu ion energy transfer. If it were, the spectral diffusion would end at about the energy relaxation time T_1, which is 2 ms for Eu^{3+}:$YAlO_3$, and would not be affected by a static magnetic field. The low concentration of Eu ions in the crystal also argues against a role for Eu-Eu energy transfer.

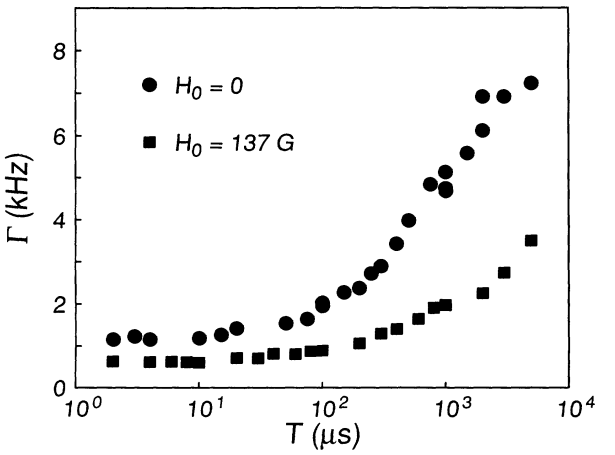

FIG. 4. Homogeneous linewidth Γ dependence on the second-to-third pulse separation T in Eu^{3+}:$YAlO_3$ at ~5.5 K with and without a static magnetic field.

We believe that the spectral diffusion is caused by the slow flip of the nearby Al nuclear spins which surround Eu^{3+} ions,[17,27,39] and that the magnetic field only slows down these flip rates by removing the degeneracies of the Al quadrupole-split levels and making the energy-conserving flip flop less probable, and the maximum extra linewidth $\Gamma^0_{SD}=\Gamma(T\rightarrow\infty)-\Gamma(T\rightarrow 0)$ caused by spectral diffusion will not be changed by a static magnetic field. Since the energy of the magnetic dipole interaction between a Eu^{3+} ion and the nearby Al nuclear spins are of kHz order and Γ^0_{SD} with $H_0=0$ is also on the order of kHz (see Fig. 4), the above idea seems reasonable.

Finally, the lengthened intrinsic dephasing time may be interpreted in the following way. The magnetic field removes the degeneracies of the bulk Al quadrupole-split levels and the energy-conserving flip flop of the bulk Al spins becomes less probable,[48] and the intrinsic dephasing time becomes longer.

IV. THEORY

Since SPE is equivalent to time-resolved spectral hole burning with the burn-to-probe time separation T, and the homogeneous linewidth Γ corresponds to $\frac{1}{2}$ of the hole width (FWHM),[39] we treat the experimental results in the spectral-hole-burning picture throughout this theory section.

Three theoretical models will be presented to explain spectral diffusion in Eu^{3+}:$YAlO_3$. In each case we write Γ in the following form:

$$\Gamma(T)=\Gamma_1+\Gamma_2(T)\ , \tag{1}$$

where Γ_1 equals to the intrinsic homogeneous linewidth $\Gamma(T\rightarrow 0)$ and $\Gamma_2(T)$ is the extra linewidth caused by spectral diffusion at time T. Equation (1) assumes that the broadening caused by spectral diffusion has a Lorentzian profile, otherwise the echo decay curve is not a single exponential decay. The time dependence of $\Gamma_2(T)$ may differ between $H_0=0$ and $H_0=137$ G, but its maximum extra linewidth $\Gamma^0_{SD}=\Gamma_2(T\rightarrow\infty)$ does not change (see previous section).

A. Bai-Fayer theory

Starting from the four-point correlation function,[50] Fayer and collaborators developed a theory of optical dephasing phenomena for chromophores in glasses that includes the effect of local configurational changes of materials.[24–28] They showed theoretically and experimentally that TPPE yields intrinsic dephasing time and that

other line narrowing experiments are sensitive to $\sim 1/T_2(T\rightarrow 0)$ rate fluctuations and slow dynamical processes occurring within the time scale of the experiments.

Bai and Fayer extended their theory in a more general form and also applied it to the spectral diffusion phenomenon in Pr^{3+}:CaF_2.[27] In that case, spectral diffusion is caused by the flip of the nearby F nuclear spins which surround a Pr^{3+} ion. The Pr^{3+} ion has a strong ground-state magnetic moment and a very weak excited-state magnetic moment. This causes the nearby F nuclear spins to form a frozen core when the Pr^{3+} ion is in the ground state.[27,40] In Bai and Fayer's treatment, they have to make a complicated correlation function to include these factors.

In the case of Eu^{3+}:$YAlO_3$, the magnitude of the magnetic moments of both $^{151}Eu^{3+}$ and $^{153}Eu^{3+}$ ions in the excited and ground states are roughly of the same order.[46] We assume for simplicity that the nearby Al nuclear spins form a frozen core and flip in the same manner whether the Eu^{3+} ion is in the excited state or in the ground state. We further assume that all the nearby Al nuclear spins only change their expectation value $+1$ or -1, and that they flip randomly at the same rate. These assumptions avoid the complicated correlation function approach used by Bai and Fayer.

With the above assumptions, Γ is expressed by the following simple equation:

$$\Gamma(T)=\Gamma_{B1}+\Gamma_{B2}[1-\exp(-RT)] , \quad (2)$$

where Γ_{B1} is the intrinsic homogeneous linewidth, Γ_{B2} is the maximum extra linewidth caused by spectral diffusion, and R is the flip rate of the nearby Al nuclear spins. Equation (2) is an accurate approximation in the limit $1/R$, $T\gg T_2(T\rightarrow 0)$.[27] The fitting procedure of Eq. (2) to the data is as follows: We first choose $\Gamma_{B1}=1.2$ kHz and least-squares fit Eq. (2) to the data with $H_0=0$. The result is $\Gamma_{B2}=6.0$ kHz and $R=1.1\times 10^3$ Hz. For $H_0=137$ G, we set $\Gamma_{B1}=0.61$ kHz and fit Eq. (2) to the data. The flip rate $R=1.6\times 10^2$ Hz for $H_0=137$ G. The value Γ_{B2} is the same for both cases.

Figure 5 shows the fitted curves and the data with and without the static magnetic field. Although the agreement of the curve and the data at $H_0=137$ G is not good, the agreement of those at $H_0=0$ is excellent in spite of the simplification used to describe the spectral diffusion phenomenon. Assuming the functional form of Eq. (2) for this phenomenon, the following conclusions are derived: The nearby Al nuclear spins flip at an almost the same rate $\sim$ kHz and this rate is slowed down roughly a factor of 7 at $H_0=137$ G (see Table I).

B. Diffusion theory

The one-dimensional diffusion equation with diffusion coefficient D and initial condition $f(x, t=0)=\delta(x)$,

$$\frac{\partial}{\partial t}f(x,t)=D\frac{\partial^2}{\partial x^2}f(x,t) , \quad (3)$$

has the solution

$$f(x,t)=(4\pi Dt)^{-1/2}\exp(-x^2/4Dt) . \quad (4)$$

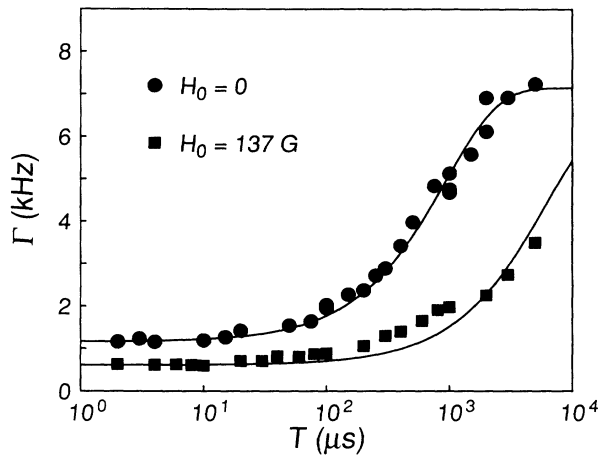

FIG. 5. Homogeneous linewidth Γ measured (● and ■) and calculated according to Bai-Fayer theory [Eq. (2)].

In this case, the root-mean-square deviation $\Delta x\propto\sqrt{t}$. When Eq. (4) is applied to the spectral diffusion phenomenon (substituting frequency ω for position x, the pulse separation T for time t), the extra linewidth caused by spectral diffusion is proportional to $\sqrt{T}$. This model, however, has two major problems:

(1) The solution (4) has a Gaussian form. Since the convolution of a Lorentzian and a Gaussian is not a Lorentzian, Eq. (4) is inconsistent with the observed single exponential decay of photon echoes.

(2) The homogeneous linewidth Γ goes to infinity at $t\rightarrow\infty$, which is unphysical.

We assume in the following that the temporal behavior of the extra linewidth caused by spectral diffusion can be modeled by Eq. (4) and is proportional to $\sqrt{T}$ when T is not large. Here Γ is written as

$$\Gamma(T)=\Gamma_{D1}+\Gamma_{D2}\sqrt{T/T_0} , \quad (5)$$

where Γ_{D1}, Γ_{D2}, and $1/T_0$ are fitting parameters, and $1/T_0$ may be proportional to the Al nuclear spin-flip rate.

The fitting procedure is the same as that for Eq. (2). With $H_0=0$, we fitted the data for $T=2$ μs to 2 ms to Eq. (4). The result is shown in Fig. 6. The fitting param-

TABLE I. Al flip rates with and without a static magnetic field.

Magnetic field (G)	Al flip rate (Hz) Bai-Fayer theory	Diffusion theory	Monte Carlo theory
0	1.1×10^3	(2.7×10^3)	2.6×10^2
137	1.6×10^2	(3.0×10^2)	26
Ratio of flip rates[a]	~ 7	~ 9	~ 10

[a]The ratio of flip rates is given by $(\text{flip rate})_{H_0=0}/(\text{flip rate})_{H_0=137\text{ G}}$.

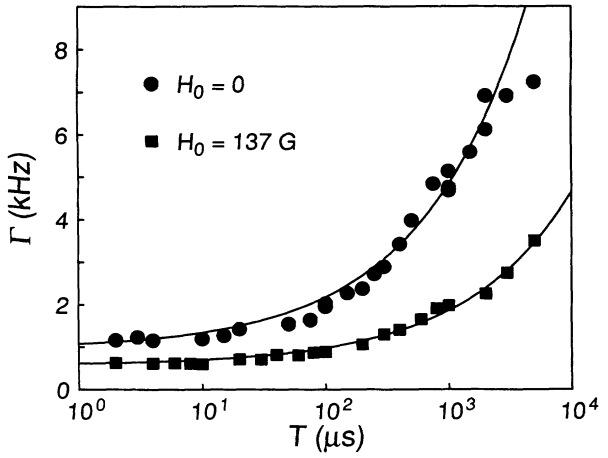

FIG. 6. Homogeneous linewidth Γ measured (● and ■) and calculated according to diffusion theory [Eq. (5)].

eters are $\Gamma_{D1}=0.96$ kHz, $1/T_0=2.7\times10^3$ Hz for $H_0=0$, and $\Gamma_{D1}=0.57$ kHz, $1/T_0=3.0\times10^2$ Hz for $H_0=137$ G. The value $\Gamma_{D2}=2.4$ kHz for both cases. In this case the agreement is better than that of Eq. (2) except for the $H_0=0$ data from $T=3$ to 5 ms. When we used intrinsic homogeneous linewidths of 1.2 kHz with $H_0=0$ and of 0.61 kHz with $H_0=137$ G for Γ_{D1}, the fitting was not good. Although $1/T_0$ does not give the actual Al nuclear spin-flip rate, the ratio of $1/T_0$ with and without the magnetic field (see Table I) gives the ratio of the Al flip rates under these conditions.

The ratio $\Gamma_{D1}/\Gamma(T\rightarrow0)$ is 0.80 with $H_0=0$, and 0.93 with $H_0=137$ G. If the Al flip rate R is slow enough and $R\ll1/T_2(T\rightarrow0)$, it will not contribute to intrinsic dephasing. If, on the other hand, the flip rate is not slow enough and $R\leq1/T_2(T\rightarrow0)$, it will contribute more or less to intrinsic dephasing. The ratio of T_0 and the intrinsic dephasing time $T_2(T\rightarrow0)$, $T_0/T_2(T\rightarrow0)$ is 1.3 with $H_0=0$ and 6.3 with $H_0=137$ G. The difference between 1.3 and 6.3 quantitatively explains the different ratios $\Gamma_{D1}/\Gamma(T\rightarrow0)$ with and without the magnetic field.

C. Monte Carlo theory

The dynamics of the nuclear spins can also be studied by the Monte Carlo method. DeVoe *et al.* demonstrated by this method that in Pr^{3+}:LaF_3, intrinsic optical dephasing arises from the local-field fluctuations due to the F nuclear spin flips.[51] Endo, Muramoto, and Hashi showed the absence of spectral diffusion in a dilute ruby Cr^{3+}:Al_2O_3 by this method.[35] Their idea is that the flip of Al nuclear spin causes the optical transition frequency shift via Cr-Al superhyperfine interaction.[35] They estimated the upper limit of the neighboring Al nuclei flip rate to be a few Hz and found that these nuclei form a frozen core.

In the case of Eu^{3+}:$YAlO_3$, the Hamiltonians which include superhyperfine interaction have not been obtained. We assume in the following:

(1) Eight nearest-neighbor Al nuclear spins form a frozen core by the perturbed electric field gradient, considering the studies of photon-echo nuclear double resonance in Eu^{3+};$YAlO_3$ (Ref. 41) and Al NMR in $YAlO_3$.[42]

(2) Eight nuclear spins flip at the same rate R randomly whether the Eu^{3+} ion is in the excited state or the ground state. For $k=1-8$, each spin state takes an up or down state, which we write $S(k)=\frac{1}{2}$ or $-\frac{1}{2}$.

(3) The magnitude of the frequency shift of a Eu^{3+} ion is the same for all Al spins. This means that the frequency shift $\Delta\omega$ is proportional to the sum of the differences $\Delta S(k)$ between the kth Al nuclear spins at time T and $T=0$.

The procedure is as follows: The first stage is the initialization of eight spin states $S(k)$ with $k=1-8$ for each ensemble (ensemble number = 2700). The $S(k)$ values take the values $+\frac{1}{2}$ or $-\frac{1}{2}$ randomly. Then the Al spin states at 10 000 discrete times are determined using a Monte Carlo method with all spin flipping at a rate R. For every time T, the total frequency shift $\Delta\omega$ for each ensemble is given by

$$\Delta\omega\propto\sum_{k=1}^{8}\Delta S(k)\ . \tag{6}$$

Since the number of Al spins is small, the distribution of $\Delta\omega$ is not necessarily a Lorentzian or a Gaussian. We assume that the temporal behavior of spectral diffusion is expressed by the root of the second moment $[(\Delta\omega)^2]^{1/2}$, and its magnitude is a parameter chosen so as to agree with the data. The second moment $(\Delta\omega)^2$ is given by

$$(\Delta\omega)^2\propto\left\langle\sum_{k=1}^{8}[\Delta S(k)]^2\right\rangle\ , \tag{7}$$

where $\langle\ \rangle$ represents an ensemble average and it is assumed that spin states k and k' ($k\neq k'$) are uncorrelated. We write the normalized function of $[(\Delta\omega)^2]^{1/2}$ as $f_s(T,R)$. Then Γ is written as

$$\Gamma(T)=\Gamma_{M1}+\Gamma_{M2}f_S(T,R)\ , \tag{8}$$

where Γ_{M1}, Γ_{M2}, and R are fitting parameters.

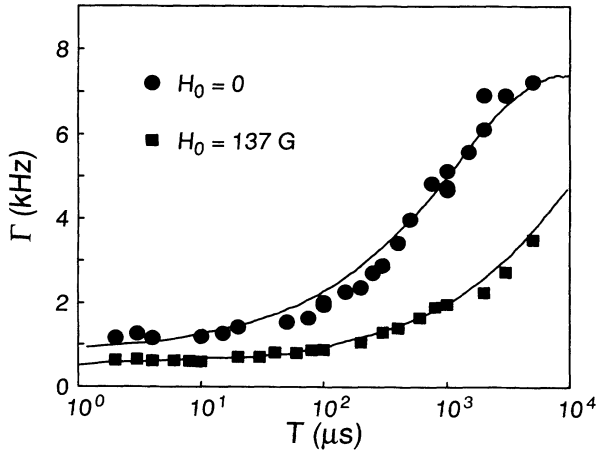

FIG. 7. Homogeneous linewidth Γ measured (● and ■) and calculated according to Monte Carlo theory [Eq. (8)].

The results of fitting to the experimental data is shown in Fig. 7. The parameters are $\Gamma_{M1}=0.96$ kHz, and $R=2.6\times10^2$ Hz for $H_0=0$, $\Gamma_{M1}=0.57$ kHz, and $R=26$ Hz for $H_0=137$ G. The value $\Gamma_{M2}=6.6$ kHz for both cases. The flip rates R with $H_0=0$ and 137 G and their ratios are given in Table I. The ratio $\Gamma_{M1}/\Gamma(T\rightarrow0)$ is 0.70 with $H_0=0$, and 0.82 with $H_0=137$ G. These differences can also be explained in a similar way as in the case of diffusion theory. Although the flip rate R differs somewhat between the Bai-Fayer and Monte Carlo theories, all the three theories show that the flip rate is sub-kHz order with $H_0=0$ and is slowed down by an order of magnitude at $H_0=137$ G.

V. CONCLUSIONS

We have performed stimulated photon-echo spectroscopy in the $^7F_0$-$^5D_0$ transition of Eu^{3+}:$YAlO_3$ at low temperatures by varying pulse separations τ and T systematically. Both the intrinsic dephasing time $T_2(T\rightarrow0)$ and the spectral diffusion rate R were affected by a static magnetic field. The sub-kHz order homogeneous linewidth obtained with $H_0=137$ G is, to our knowledge, the narrowest ever reported.

The origin of spectral diffusion is attributed to the flip of the nearby Al nuclear spins which surround a Eu^{3+} ion. Assuming that all the nearby Al nuclear spins flip at the same rate, that the magnetic field slows down the Al flip rate, and that the maximum extra linewidth caused by spectral diffusion is constant, the homogeneous linewidth as a function of the second-to-third pulse separation was calculated according to Bai-Fayer theory, diffusion theory, and Monte Carlo theory. Reasonably good agreements between measured homogeneous linewidths and calculated curves were obtained for each theory. The closest agreement was obtained using diffusion theory, but this theory gives unphysical results when T is large. Both Bai-Fayer theory and Monte Carlo theory, on the other hand, give more physical results and can be applied to more complicated cases.

Although the flip rate of the nearby Al nuclear spins surrounding a Eu^{3+} ion differs between the Bai-Fayer and Monte Carlo theories, all three theories show that the flip rate is sub-kHz order at $H_0=0$ and is slowed down by an order of magnitude at $H_0=137$ G.

ACKNOWLEDGMENT

We thank Dr. Tetsuo Ogawa for valuable discussions.

[1]D. Grischkowsky and S. R. Hartmann, Phys. Rev. B **2**, 60 (1970).
[2]S. Nakanishi, O. Tamura, T. Muramoto, and T. Hashi, Jpn. J. Appl. Phys. **19**, L57 (1980).
[3]R. M. Macfarlane, C. S. Yannoni, and R. M. Shelby, Opt. Commun. **32**, 101 (1980).
[4]Y. C. Chen, K. Chang, and S. R. Hartmann, Phys. Rev. B **21**, 40 (1980).
[5]M. K. Kim and R. Kachru, Phys. Rev. B **40**, 2082 (1989).
[6]M. Mitsunaga, R. Yano, and N. Uesugi, following paper, Phys. Rev. B **45**, 12 760 (1992).
[7]T. W. Mossberg, Opt. Lett. **7**, 77 (1982).
[8]Y. S. Bai, W. R. Babbitt, and T. W. Mossberg, Opt. Lett. **11**, 724 (1986).
[9]M. K. Kim and R. Kachru, J. Opt. Soc. Am. B **4**, 305 (1987).
[10]M. Mitsunaga and N. Uesugi, Opt. Lett. **15**, 195 (1990).
[11]A. Rebane and O. Ollikanen, Opt. Commun. **78**, 327 (1990).
[12]R. M. Macfarlane and R. M. Shelby, in *Spectroscopy of Solids Containing Rare Earth Ions,* edited by A. A. Kaplyanskii and R. M. Macfarlane (North-Holland, Amsterdam, 1987).
[13]A. Renn, A. J. Meixner, U. P. Wild, and F. A. Burrhalter, Chem. Phys. **93**, 157 (1985).
[14]A. J. Meixner, A. Renn, and U. P. Wild, J. Chem. Phys. **91**, 6728 (1989).
[15]M. J. Weber, in *Laser Spectroscopy of Solids,* edited by W. M. Yen and P. M. Selzer (North-Holland, New York, 1981).
[16]T. Muramoto, S. Nakanishi, and T. Hashi, Opt. Commun. **24**, 316 (1978).
[17]R. M. Shelby and R. M. Macfarlane, J. Lumin. **31&32**, 839 (1984).
[18]W. H. Hesselink and D. A. Wiersma, Phys. Rev. Lett. **43**, 1991 (1979).
[19]S. Asaka, H. Nakatsuka, M. Fujiwara, and M. Matsuoka, Phys. Rev. A **29**, 2286 (1984).
[20]N. Morita and T. Yajima, Phys. Rev. A **30**, 2525 (1984).
[21]R. Beach and S. R. Hartmann, Phys. Rev. Lett. **43**, 663 (1984).
[22]T. Kobayashi, T. Hattori, A. Terasaki, and K. Kurokawa, Rev. Phys. Appl. **22**, 1773 (1987).
[23]H. Nakatsuka, Y. Matsumoto, K. Inouye, and R. Yano, Opt. Lett. **14**, 633 (1989).
[24]M. Berg, C. A. Walsh, L. R. Narashimhan, and M. D. Fayer, J. Lumin. **38**, 9 (1987).
[25]M. Berg, C. A. Walsh, L. R. Narashimhan, K. A. Littau, and M. D. Fayer, J. Chem. Phys. **88**, 1564 (1988).
[26]Y. S. Bai and M. D. Fayer, Chem. Phys. **128**, 135 (1988).
[27]Y. S. Bai and M. D. Fayer, Phys. Rev. B **39**, 11 066 (1989).
[28]Y. S. Bai, K. A. Littau, and M. D. Fayer, Chem. Phys. Lett. **162**, 449 (1989).
[29]W. Breinl, J. Friedrich, and D. Haarer, J. Chem. Phys. **81**, 3915 (1984).
[30]A. Rebane and D. Haarer, Opt. Commun. **70**, 478 (1989).
[31]H. Nakatsuka, K. Inouye, S. Uemura, and R. Yano, Chem. Phys. Lett. **171**, 245 (1990).
[32]*Amorphous Solids: Low Temperature Properties,* edited by W. A. Phillips (Springer, Berlin, 1981).
[33]P. W. Anderson, B. I. Halperin, and C. W. Varma, Philos. Mag. **25**, 1 (1972).
[34]W. A. Phillips, J. Low Temp. Phys. **7**, 351 (1972).
[35]T. Endo, T. Muramoto, and T. Hashi, Phys. Lett. **99A**, 128 (1983).
[36]R. Wannemacher, R. S. Meltzer, and R. M. Macfarlane, J. Lumin. **45**, 307 (1990).
[37]R. G. DeVoe, A. Szabo, S. C. Rand, and R. G. Brewer, Phys. Rev. Lett. **42**, 1560 (1979).
[38]S. C. Rand, A. Wokaun, R. G. DeVoe, and R. G. Brewer, Phys. Rev. Lett. **43**, 1868 (1979).
[39]W. M. Mims, in *Electron Paramagnetic Resonance,* edited by S. Geschwind (Plenum, New York, 1972).

[40]D. P. Burum, R. M. Shelby, and R. M. Macfarlane, Phys. Rev. B **25**, 3009 (1982).
[41]D. P. Burum, R. M. Macfarlane, and R. M. Shelby, Phys. Lett. **90A**, 483 (1982).
[42]D. P. Burum, R. M. Macfarlane, and R. M. Shelby, Phys. Lett. **91A**, 465 (1982).
[43]D. R. Taylor, J. R. Marko, and I. G. Bartlet, Solid State Commun. **14**, 295 (1974).
[44]D. R. Taylor and J. P. Hessler, Phys. Lett. **53A**, 451 (1975).
[45]J. Huang, J. M. Zhang, A. Lezama, and T. W. Mossberg, Phys. Rev. Lett. **63**, 78 (1989).
[46]R. M. Shelby and R. M. Macfarlane, Phys. Rev. Lett. **47**, 1172 (1981).
[47]T. W. Mossberg, R. Kachru, S. R. Hartmann, and A. M. Flusberg, Phys. Rev. A **20**, 1976 (1979).
[48]R. M. Macfarlane, R. M. Shelby, and R. L. Shoemaker, Phys. Rev. Lett. **43**, 1726 (1979).
[49]R. M. Shelby and R. M. Macfarlane, Phys. Rev. Lett. **45**, 1098 (1980).
[50]S. Mukamel and R. F. Loring, J. Opt. Soc. Am. B **3**, 595 (1986).
[51]R. G. DeVoe, A. Wokaun, S. C. Rand, and R. G. Brewer, Phys. Rev. B **23**, 3125 (1981).